Theoretical and Experimental Studies of Tyrosyl Hydroperoxide Formation in the Presence of H-Bond Donors

ARTICLE *in* CHEMICAL RESEARCH IN TOXICOLOGY · OCTOBER 2008

Impact Factor: 3.53 · DOI: 10.1021/tx8001687 · Source: PubMed

2 AUTHORS, INCLUDING:

Frederick A. Villamena
The Ohio State University
88 PUBLICATIONS **1,684** CITATIONS

Published in final edited form as:
Chem Res Toxicol. 2008 October ; 21(10): 1923–1932. doi:10.1021/tx8001687.

Theoretical and Experimental Studies of Tyrosyl Hydroperoxide Formation in the Presence of H-bond Donors

Steven M. Field and **Frederick A. Villamena***
Department of Pharmacology and Davis Heart and Lung Research Institute, College of Medicine The Ohio State University, Columbus, Ohio, 43210 USA

Abstract

Oxidative damage to biomolecules such as lipids, proteins, nucleotides and sugars has been implicated in the pathogenesis of various diseases. Superoxide radical anion ($O_2^{\bullet-}$) addition to nitrones bearing an amide N-H has been shown to be more favored compared to other nitrones (Villamena, F. A., et al., *J. Am. Chem. Soc*., **2007**, *129*, 8177–8191). It has also been demonstrated by others (Winterbourn, C. C., et al., *Biochem. J*. **2004**, *381*, 241–248) that $O_2^{\bullet-}$ addition to tyrosine to form hydroperoxide is favored in the presence of basic amino groups but the mechanism for this observation remains obscure. We, therefore, hypothesized that the α-effect resulting from the interaction of $O_2^{\bullet-}$ with N-H can play a crucial role in the enhancement of hydroperoxide formation. Understanding this phenomenon is important in the elucidation of mechanisms leading to oxidative stress in cellular systems. Computational (PCM/B3LYP/6-31+G**//B3LYP/6-31G level of theory) as well as experimental studies were carried out to shed insights into the effect of amide or amino N-H on the enhancement (or stabilization) of hydroperoxide formation in tyrosine. H-bond interaction of amino acid group with $O_2^{\bullet-}$ results in the perturbation of the spin and charge densities of $O_2^{\bullet-}$. Similar phenomenon has been predicted for non-amino acids bearing H-bond donor groups. Using FOX assay, tyrosyl hydroperoxide formation was enhanced in the presence of H-bond donors from amino acids and non-amino acids. The role of H-bonding in either stabilizing the hydroperoxide adduct, or facilitation of $O_2^{\bullet-}$ addition via α-effect was further theoretically investigated, and results show that the latter mechanism is more thermodynamically preferred. This study provides new mechanistic insights in the initiation of oxidative modification to tyrosyl radical.

Introduction

Reactive oxygen species, such as superoxide radical anion ($O_2^{\bullet-}$), have been shown to play a crucial role in modulating cell function, signaling, and immune response (1). However, production of $O_2^{\bullet-}$ can be induced through various chemical, enzymatic, or biological means (2–4) and in unregulated concentrations, $O_2^{\bullet-}$ can be a major source of the most highly oxidizing species known to exist in biological systems such as peroxynitrite ($ONOO^-$), oxidized glutathione radical anion ($GSSG^{\bullet-}$), hypochlorous acid (HOCl), carbonate radical anion ($CO_3^{\bullet-}$), or hydroxyl radical ($HO^{\bullet}$) (1). Superoxide is not highly reactive in spite of its free radical nature but its selective reactivity with other radical species (e.g., NO, tyrosyl radical) and transition metal ions such as Fe(II) (5) makes $O_2^{\bullet-}$ one of the toxic radical species in biological system.

In our efforts to develop spin traps with improved properties for analytical and therapeutic applications (6–11), we have demonstrated that nitrones with an amide substituent, e.g., 5-carbamoyl-5-methyl-pyrroline *N*-oxide (AMPO), exhibit higher reactivity towards $O_2^{\bullet-}$

*To whom correspondence should be addressed: frederick.villamena@osumc.edu; Tel. No. 614-292-8215; Fax: 614-688-0999.

compared to other known spin traps such as 5,5-dimethyl-pyrroline *N*-oxide (DMPO), 5-diethoxyphosphoryl-5-methyl-pyrroline *N*-oxide (DEPMPO) and 5-ethoxycarbonyl-5-methyl-pyrroline *N*-oxide (EMPO). This high reactivity towards $O_2^{\bullet-}$ has been rationalized to be due to a combination of electrostatics and intra-molecular H-bonding interaction of the $O_2^{\bullet-}$ with the amide-H at the transition state of the adduct (10). This observation has given rise to more questions about the possibility that this process could also be happening in protein systems in which amide moiety is abundant, and hence, can have significant ramification in the initiation of oxidative damage to biomolecules.

Oxidative damage is prevalent in protein systems and oxidative modification has been shown to lead to loss of protein function (2,12–14). The addition of $O_2^{\bullet-}$ to the phenoxyl ($PhO^{\bullet}$) radical leading to the formation of hydroperoxide suggests a similar oxidative modification may occur in peptides or proteins with tyrosyl radical ($TyrO^{\bullet}$) group (15). Superoxide has the ability to preferentially interact with certain amino acids in biological systems such as the $TyrO^{\bullet}$ through an addition reaction to produce hydroperoxide (16–19). In addition, the formation of hydroperoxide adduct prevails over the formation of tyrosine dimers, or phenol and O_2 via electron transfer mechanism (18,19). In peptides, the efficiency of the reaction of $TyrO^{\bullet}$ to $O_2^{\bullet-}$ has been proposed to be dependent on the proximity of the tyrosyl moiety to the amino or amide groups (17). Thus, it has been suggested that hydroperoxides such as tyrosyl hydroperoxide and tyrosine dimers can be used as biomarkers of oxidative stress in a number of pathophysiological condition such as cardiovascular disease (17). $TyrO^{\bullet}$ is part of the catalytic cycle of ribonucleotide reductase (20–22), prostaglandin synthase and photosystem II (23), and is being formed from myoglobin (24) and peroxidases (25) in the presence of hydrogen peroxide. Furthermore, since modification of tyrosine moieties in proteins has been shown to result in enzyme deactivation (13), studies involving $O_2^{\bullet-}$ reaction to $TyrO^{\bullet}$ are relevant.

Experimental

a. General procedure

Tyrosyl hydroperoxide formation was generated according to the method previously described (19). In a typical experiment, a solution composed of horseradish peroxidase (HPO) (10 μg/mL), xanthine oxidase (XO) (0.05 U/mL), tyrosine (1 mM), amino acid (1 mM), and acetaldehyde (1 mM) in 10 mM phosphate buffer solution was allowed to sit at room temperature for 30–40 minutes then catalase (20 μg/mL) was added to consume any extra hydrogen peroxide. The final solution with a volume of 700 μL was allowed to sit for another 10 minutes and analyzed for hydroperoxide formation using FOX assay (18,26,27). FOX reagent is composed of 0.4 M sorbitol, 1 mM $Fe(NH_4)SO_4$, 0.4 mM xylenol orange in 0.2 M H_2SO_4, and 250 μL of this reagent was added to the 700 μL of reaction mixture. The solution was allowed to sit at room temperature for 45 minutes and absorbance reading was obtained at 560 nm. Peroxide equivalents were calculated based on cumene hydroperoxide as standard and were corrected by subtracting the absorbance readings from the mixture in the absence of tyrosine. Similar experiments were performed using non-amino acid in the presence and absence of H-bond donor groups. All experiments were done in duplicate or triplicate. The amino acids used were arginine, lysine, glycine, tryptophan, histidine, asparagine and phenylalanine. Non-amino acids used include benzylamine, aniline, acetamide, 3-amino benzoic acid, urea, benzoic acid, phenyl acetic acid, benzyl alcohol, ethanol, *N*,*N*-dimethyl formamide, *N*,*N*,*N*′,*N*′-tetramethylurea, triethylamine and 3-dimethylamino-methyl benzoate. As controls, each reaction was repeated by adding superoxide dismutase (SOD) (20 μg/mL) solution to the mixture in order to consume any superoxide that was formed and peroxide equivalents were also calculated in the presence of 2 mM amino acid or non-amino acid alone and in the absence of tyrosine. *Time dependence studies*. Same as above but 1 mM of urea was

added during the 30 min incubation period at different time points, i.e., 0, 5, 10, 15, 20, 25, and 30 min. After incubation, catalase was added and the final solution was quantified for hydroperoxide formation using FOX assay.

b. Computational Method

Conformational search was carried out using Spartan 04 (28) via a Monte Carlo method coupled with the MMFF-94 force field. Variations in energetics as a function of basis set and method was assessed using B3LYP/6-31G* geometries and single-point energies at B3LYP/6-31 +G**, B3LYP/6-311++G**, B3LYP/aug-cc-pVDZ, BHandHLYP/6-31+G**, mpw1pw91/6-31+G** and PBE1PBE/6-31+G** levels of theory. Reaction energy at the B3LYP/6-31+G**//B3LYP/6-31G* is within ~1 kcal/mol difference of the energetics calculated at the B3LYP/aug-cc-pVDZ and BHandHLYP/6-31+G** levels (see Table S1 of Supporting Information), therefore, B3LYP/6-31+G**//B3LYP/6-31G* offers a reasonable approximation to the higher-level basis set and BHandHLYP/6-31+G** which is effective in approximating barrier height energies (29,30). Density functional theory (DFT) (31,32) was applied in this study to determine the optimized geometry, vibrational frequencies, and single-point energy of all stationary points (33–36). All calculations were performed using Gaussian 03 (37) at the Ohio Supercomputer Center. Single-point energies were obtained at the B3LYP/6-31+G** level based on the optimized B3LYP/6-31G* geometries, and the B3LYP/6-31 +G**//B3LYP/6-31G* wave functions were used for Natural Population Analyses (NPA) (38). The effect of aqueous solvation was also investigated using the polarizable continuum model (PCM) (39–43). These calculations used six Cartesian d functions. Stationary points for all the optimized compounds have zero imaginary vibrational frequency as derived from a vibrational frequency analysis (B3LYP/6-31G*). A scaling factor of 0.9806 was used for the zero-point vibrational energy (ZPE) corrections for the B3LYP/6-31G* level (44). Spin contamination for all of the stationary point of the radical structures was negligible, i.e., $\langle S^2 \rangle = 0.75$.

Results and Discussion

a. Tyrosyl hydroperoxide formation with amino acids

Tyrosyl hydroperoxide formation in the presence of glycine, phenylalanine, asparagine or tryptophan as well as basic amino acids such as arginine, lysine or histidine, was experimentally investigated. Figure 1 shows that, in general, the formation of hydroperoxide was enhanced in the presence of equimolar concentrations of an amino acid (1 mM) and tyrosine (1 mM) regardless of their pK_a. Tyrosine (2 mM) alone in the absence of added amino acid resulted to hydroperoxide formation which is significantly higher compared to using other amino acids (2 mM) in the absence of tyrosine but did not exhibit the same degree of enhancement as 1 mM tyrosine with 1 mM of an amino acid (Figure 1 and Figure S1). Based on the concentrations of the amino acids used in the experiments, the amount of hydroperoxide formed from the mixture of amino acids is not additive of the hydroperoxides formed from individual amino acids, and this is further demonstrated in Figure S1 for tyrosine and arginine. These results also suggest that hydroperoxide formation can be influenced not only by the basic group of an amino acid but perhaps by any H-bond donor group originating from the amino acid moiety. The false positive results obtained from amino acids in the absence of tyrosine could arise from catalase, SOD or HRP in the mixture, but its nature is unclear at the moment and warrants further investigation. The enhanced formation of hydroperoxide in the presence of tyrosine as well as in the absence of SOD further indicate that the hydroperoxide originates from the reaction of $TyrO^{\bullet}$ and $O_2^{\bullet -}$ (Figure 1). From the seminal work of Jin et al. (45), $O_2^{\bullet -}$ was shown to react with $TyrO^{\bullet}$ to form the hydroperoxide adduct with a rate constant of 1.5×10^9 M^{-1} s^{-1} and its subsequent decay ($t_{1/2}$ = 4.2 h) leads to the formation of the bicyclic compound **1**. Evidence for hydroperoxide formation has also been previously reported (13,15–17,19,45).

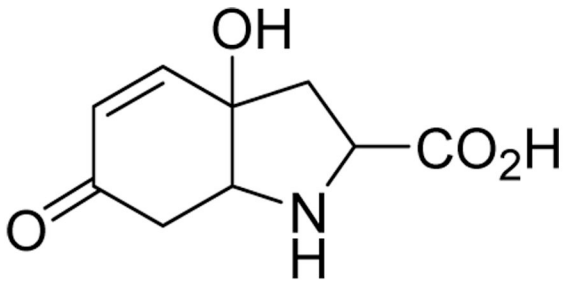

1

Figure 2 shows that the amount of hydroperoxide formed increases with increasing concentration of tyrosine, acetaldehyde or arginine. The transition state structure of the hydroperoxide formed could involve participation of three major species, i.e., $TyrO^{\bullet}$, $O_2^{\bullet-}$ and an H-bond donor, since the amount of hydroperoxide formed is dependent on tyrosine, acetaldehyde and arginine concentration, respectively. Winterbourn, et al. (19) had proposed that the increased hydroperoxide formation in the presence of basic amino acid is due to the formation of a stable amino hydroperoxide via Michael addition reaction of the amino group to the tyrosyl peroxide intermediate.

In a separate study, we observed a similar phenomenon in which there is an increased favorability of $O_2^{\bullet-}$ addition to nitrones in the presence of amide substituent compared to methyl, ester or phosphoryl substituents (9). We later concluded that factors such as intramolecular H-bonding of $O_2^{\bullet-}$ in the transition state and electrostatic effects facilitate the $O_2^{\bullet-}$ adduct formation (10). This increased rate in hydroperoxide formation in nitrones bearing an amide moiety was suggested to be due to the α-effect (46) as shown by the presence of intramolecular H-bonding interaction between the amide hydrogen and the superoxide oxygen in the transition state. Alpha-effect is exhibited by a class of nucleophiles which have an electronegative atom (with one or more lone-pair of electrons) adjacent to the nucleophilic center called **α**-nucleophiles (46,47). Alpha-nucleophiles tend to be very strong electron donors, and yet are very weak bases due to the inductive effect of the heteroatom adjacent to it. This high activity is due to the repulsive interactions between the unshared electron pairs on adjacent atoms between the lone-pair of electrons on the **α**-atom and those on the nucleophilic center. This makes an **α**-nucleophile unstable and hence more reactive (46).

We therefore hypothesized that the presence of H-bond donors, in general, may affect the rate of $O_2^{\bullet-}$ addition to $TyrO^{\bullet}$ in which the $O_2^{\bullet-}$ H-bonding interaction with amino acids may modify its reactivity similar to that of hydroperoxyl radical ($HO_2^{\bullet}$). Table 1 shows the spin and charge density distributions on the $O_2^{\bullet-}$ and $HO_2^{\bullet}$, and their short O-O bond distances of 1.33 Å are characteristics of a pi-radical. By virtue of symmetry, the charge and spin density distribution on the two oxygen atoms of $O_2^{\bullet-}$ are equivalent, but addition of a proton to one of the oxygens to form $HO_2^{\bullet}$ perturbs the electronic and charge distribution between the two oxygen atoms resulting in higher spin density on the terminal oxygen atom (73%) compared to the oxygen atom (35%) bound to the hydrogen atom. This polarization in the charge and spin density distribution in $HO_2^{\bullet}$ can have significant effect on its reactivity as shown by the difference in the reduction potentials between $O_2^{\bullet-}$ and $HO_2^{\bullet}$ of $E^{o\prime} = 0.94$ and 1.06 V, respectively, in which the latter is more oxidizing than the former (48).

Based on the premise that the $O_2^{\bullet-}$ interaction with an H-bond donor would perturb its electronic property, and hence, would assume a similar reactivity to that of $HO_2^{\bullet}$ (see Table 1 for the spin and charge densities of $O_2^{\bullet-}$ versus $HO_2^{\bullet}$), we calculated the thermodynamics of

$O_2^{\bullet-}$ complex formation with various amino acids at the PCM/B3LYP/6-31+G**//B3LYP/6-31G* level of theory. Figure 3 shows the various modes of intermolecular interaction of $O_2^{\bullet-}$ with arginine and lysine exhibiting strong H-bond interactions from the amino, carboxylic acid, guanidinium hydrogens (see Figure S2 for other amino acid-$O_2^{\bullet-}$ complexes). These H-bonding interactions result in significant perturbation of the spin and charge densities of the $O_2^{\bullet-}$ as shown in Table 1, except for His---$O_2^{\bullet-}$ and Arg---$O_2^{\bullet-}$ complexes (in which the charge densities were perturbed but not the spin densities) due perhaps to the competing H-bond interaction of the amino group with the carboxylic acid for the $O_2^{\bullet-}$. Nevertheless, the low endoergicity of the free energies and exoergicity of the enthalpies of complexation of $O_2^{\bullet-}$ with amino acids may translate to a favorable complex formation in solution. The perturbation of the electronic properties of $O_2^{\bullet-}$ could be due to acid-base reaction since proton transfer reaction from the ammonium and carboxylic acid to $O_2^{\bullet-}$ was observed for Lys---$O_2^{\bullet-}$ and Gly---$O_2^{\bullet-}$ complexes, respectively. However, proton transfer was not observed for other amino acid---$O_2^{\bullet-}$ complexes but still shows the same perturbation in the electronic properties of $O_2^{\bullet-}$ suggesting that H-bond interaction plays a major role in altering the electron density distribution on $O_2^{\bullet-}$ (see Figure S2).

A similar complexation phenomenon was observed for 1-methyl-1-carbamoylcyclopentane (MCCP) and $O_2^{\bullet-}$ with a calculated $\Delta G_{rxn,298K,aq}$ and $\Delta H_{rxn,298K,aq}$ of −4.1 and 4.7 kcal/mol, respectively, and an experimental rate constant of 2.0 M^{-1} s^{-1} in DMF (10) which is far less than the rate constant observed for the tyrosyl radical dimer formation of 4.5×10^8 M^{-1} s^{-1} (45). Therefore, the rate of $O_2^{\bullet-}$ complexation may not be competitive towards TyrO$^\bullet$ dimerization but upon consideration of the relative concentrations of the H-bond donating amino acids and non-amino acids used in this study versus the TyrO$^\bullet$ concentration present in solution, the latter is expected to be in the orders of magnitude lower than the mM concentrations of the H-bond donors due to the short half-life of TyrO$^\bullet$. Moreover, based on the typical yield of the tyrosyl hydroperoxide (< 2 μM) and the rate constant of $O_2^{\bullet-}$ addition to TyrO$^\bullet$ of 1.5×10^9 M^{-1} s^{-1} (45), the initial concentration of TyrO$^\bullet$ formed is expected to be in the same concentration range as the tyrosyl hydroperoxide. Since the half life of TyrO$^\bullet$ in ribonucleotide reductase is in days (49) the low rate constant for the -NH----$O_2^{\bullet-}$ complex formation can facilitate $O_2^{\bullet-}$ addition to TyrO$^\bullet$ similar to the electrostatic guidance that Koppenol (50) had suggested to explain the efficiency of superoxide dismutase (SOD) selectivity for $O_2^{\bullet-}$ (51). Moreover, Fridovich (51) had pointed out that ionic strength effect (52,53) and site-specific modification (54) can affect the specificity and activity of SOD, respectively. It was also previously shown (19) that there is an increase in tyrosyl hydroperoxide formation in peptides containing an amino group such as lysine that is adjacent to the tyrosyl group. The same enhancement in tyrosyl hydroperoxide formation was observed in the presence of free lysine or ethanolamine (19). It is therefore, reasonable to assume that -NH----$O_2^{\bullet-}$ complex formation may play an important role in the facilitation and selectivity of $O_2^{\bullet-}$ addition to TyrO$^\bullet$ in protein systems especially when these H-bond donors are in close proximity to the TyrO$^\bullet$ group.

Figure S3 of the Supporting Information shows a comparison of the energetics of the various modes of $O_2^{\bullet-}$ and $HO_2^\bullet$ addition to TyrO$^\bullet$, and results show that the ortho addition was the most exoergic with $\Delta G_{rxn,aq,298K}$ of −6.8 kcal/mol (Figure 4) compared to the endoergic para and meta addition with $\Delta G_{rxn,aq,298K}$ of 16.3 and 19.9 kcal/mol, respectively. Addition of $HO_2^\bullet$ however to TyrO$^\bullet$ at the ortho and para positions are the most exoergic with $\Delta G_{rxn,aq,298K}$ of −11.5 and −11.8 kcal/mol, respectively, with the meta addition being the least favorable with $\Delta G_{rxn,aq,298K}$ of 19.1 kcal/mol. Ortho and para addition of $O_2^{\bullet-}$ to TyrO$^\bullet$ have been previously proposed (45) but the former is more likely to be formed in solution based on their relative energetics. Figure 4 shows the spin and charge distribution on the TyrO$^\bullet$ indicating that the carbon atom para to the amino acid group has the most positive charge (0.37 e) while the carbon to which the amino group is attached to has the highest spin density distribution of

0.35 e. Because the ortho carbon of TyrO$^{\bullet}$ has relatively high spin density and negative charge compared to other carbon atoms in the aromatic ring (Figure 4), and that the preferred site of $O_2^{\bullet-}$ and $HO_2^{\bullet}$ addition to TyrO$^{\bullet}$ is at the ortho position, suggest that the nature of $O_2^{\bullet-}$ and $HO_2^{\bullet}$ addition to TyrO$^{\bullet}$ is electrophilic in nature.

As shown in Figure 1, the significantly higher hydroperoxide formed from 2 mM tyrosine alone compared to using 2 mM of an amino acid in the absence of tyrosine could be due to the direct addition of $O_2^{\bullet-}$ to TyrO$^{\bullet}$ or $HO_2^{\bullet}$ to TyrO$^{\bullet}$ according to Scheme 1, Reactions A and G-H, respectively. Proton abstraction by $O_2^{\bullet-}$ from the carboxylic acid moiety to give $HO_2^{\bullet}$ (Reaction G) has $\Delta G_{rxn,aq,298K}$ of 0.0 kcal/mol and that direct addition of $HO_2^{\bullet}$ to the unprotonated (Reaction H) and protonated (Reaction F) TyrO$^{\bullet}$ gave exoergic reaction energies of −6.8 and −11.5 kcal/mol, respectively. Since the hydroperoxide formation experiments were performed in neutral pH, and that the known pK_a for $HO_2^{\bullet}$ is 4.8 (55) and 4.4 (56) and that of tyrosine is 2.2, the addition of $HO_2^{\bullet}$ to unprotonated TyrO$^{\bullet}$ via Reactions G-H is more likely to occur than Reaction F. However, since Reactions G-H which involve initial acid-base reaction to form $HO_2^{\bullet}$, hydroperoxide formation from this mechanism should be independent of the nature of the amino acid and should yield similar amounts of hydroperoxide from using 2 mM of tyrosine alone to that using 1 mM of tyrosine in the presence of added 1 mM amino acid. Since tyrosine in the presence of added amino acid yielded hydroperoxide that is significantly higher than tyrosine alone, Reaction A could be a more plausible mechanism and that the added amino acid plays a role in hydroperoxide formation most likely via α-effect as mentioned above. Other pathways for $O_2^{\bullet-}$ reaction to TyrO$^{\bullet}$ was also considered and are shown in Scheme 1. The oxidation of $O_2^{\bullet-}$ by TyrO$^{\bullet}$ via electron transfer mechanism (Reaction D) is exoergic with $\Delta G_{rxn,aq,298K}$ = −5.7 kcal/mol compared to its endoergic reduction to peroxide (Reaction E) with $\Delta G_{rxn,aq,298K}$ = 82.3 kcal/mol with the former only leading to the formation of phenoxide and oxygen. Although Reaction D is favorable, the formation of hydroperoxide is competitive enough to be observed experimentally.

b. Tyrosyl hydroperoxide formation with non-amino acids

To further verify the role of H-bonding on the formation of hydroperoxide, non-amino acids with a variety of H-donor groups were used. Compounds with -NH_2 group (e.g., benzylamine, aniline, acetamide, and urea) as well as compounds with –COOH group (e.g., benzoic acid, phenylacetic acid) as potential H-bond donors were assessed for their ability to enhance hydroperoxide formation in the presence or absence of SOD, as well as in the absence of tyrosine. Similar to the observation made in the presence of added amino acid, an increase in tyrosyl hydroperoxide formation was observed compared to when these non-amino acids are not present as shown in Figure 6. Moreover, hydroperoxide formation is minimal in the absence of tyrosine. Compounds with –OH group such as ethanol and benzyl alcohol also exhibited enhancement of hydroperoxide formation but not to the same degree of enhancement as observed for the –NH_2 and –COOH bearing compounds. Figure 6 therefore suggests that regardless of the nature of the H-bond donors, i.e., amine, amide, carboxylic acid, or alcohol, that the formation of hydroperoxide is dependent on the presence of H-bond donors.

The high concentration of tyrosyl hydroperoxide formed in the presence of H-bond donors led us to rationalized that H-bond interaction with $O_2^{\bullet-}$ can increase the amount of tyrosyl hydroperoxide formed due to the perturbation of $O_2^{\bullet-}$ electron density (Figure 6 and Figure 7). We therefore further focused our investigation on urea due to its biological relevance. Theoretical calculation at the PCM/B3LYP/6-31+G**//B3LYP/6-31G* level of theory was performed on the $O_2^{\bullet-}$ complex formed with urea, acetamide and *N*,*N*-dimethylacetamide to investigate if H-bonding will perturb the electronic property of $O_2^{\bullet-}$. Figure S4 shows that $O_2^{\bullet-}$ complex formation via H-bonding with urea and acetamide is less endoergic ($\Delta G_{rxn,aq,298K}$ = 5–;7 kcal/mol) compared to $O_2^{\bullet-}$ complex formation with *N*,*N*-dimethylated

acetamide ($\Delta G_{rxn,aq,298K}$ = 11.4 kcal/mol). Urea and acetamide can polarize the charge and spin density distribution of $O_2^{\bullet-}$ upon complexation provided that only one end of the $O_2^{\bullet-}$ is H-bonded. The same behavior was also predicted for benzyl alcohol and ethanol in which their complex formation with $O_2^{\bullet-}$ gave $\Delta G_{rxn,aq,298K}$ = 7.2−7.3 kcal/mol (Figure S4) with polarization of the $O_2^{\bullet-}$ electronic distribution. However, there was negligible change in the spin and charge densities on $O_2^{\bullet-}$ and *N*,*N*-dimethyl acetamide complex which is supported by the experimentally observed low hydroperoxide formation in the presence of *N*,*N*-dimethyl acetamide (Figure 7). Hydroperoxide formation using non-H-bond donating compounds (Figure 7) is significantly lower relative to using H-bond donating compounds which further suggests that intermolecular H-bond interaction plays a critical role in the enhanced formation of tyrosyl hydroperoxide similar to that observed in the presence of amino acids.

c. Alpha effect versus stabilization of the tyrosyl hydroperoxide formation in the presence of urea

In order to investigate the effect of urea on the thermodynamics of $O_2^{\bullet-}$ addition to TyrO$^{\bullet}$, the free energy of reaction of urea- $O_2^{\bullet-}$ complex to TyrO$^{\bullet}$ was calculated and compared to the energetics of addition of $O_2^{\bullet-}$ to TyrO$^{\bullet}$ in the absence of urea (Scheme 1, Reactions A versus C). Figure 5 shows that the most preferred mode of urea---$O_2^{\bullet-}$ addition is at the ortho position with $\Delta G_{rxn,aq,298K}$ = −3.7 kcal/mol compared to the para- and meta- addition with $\Delta G_{rxn,aq,298K}$ of −1.7 and 23.0 kcal/mol, respectively (Figure S5). The preference for urea---$O_2^{\bullet-}$ to add at the ortho position is similar to that predicted for $O_2^{\bullet-}$ addition to TyrO$^{\bullet}$ alone. However, addition of urea---$O_2^{\bullet-}$ is exoergic by −3.7 kcal/mol but is less exoergic by 3.0 kcal/mol than the addition of $O_2^{\bullet-}$ alone, indicating that α-effect from the amino acid moiety may already have played a role in facilitating $O_2^{\bullet-}$ addition but experimental results show that 1 mM tyrosine in the presence of 1 mM urea gave significantly higher hydroperoxide yield compared to 2 mM tyrosine (Figure 7) suggesting that urea plays a role in facilitating hydroperoxide formation. A more obvious effect of urea can be seen on the urea---$O_2^{\bullet-}$ addition at the para position with a $\Delta G_{rxn,aq,298K}$ of −1.7 compared to 16.3 kcal/mol in the absence of urea (Figure S5).

To further prove that the amino acid group plays a role in facilitating $O_2^{\bullet-}$ addition, the effect of amino acid group was eliminated by investigating the energetics of addition of $O_2^{\bullet-}$ versus urea---$O_2^{\bullet-}$ to the phenoxyl radical only (Figure 5 and Figure S6). The free energies of $O_2^{\bullet-}$ addition to PhO$^{\bullet}$ at the para, meta and ortho positions are 1.8, 19.5, and 7.0 kcal/mol, respectively, while addition of urea---$O_2^{\bullet-}$gave more favorable energies with $\Delta G_{rxn,aq,298K}$ of 0.5, −15.5 and 3.5 kcal/mol for para, meta and ortho additions, respectively. Therefore, a more consistent trend in the energetics of $O_2^{\bullet-}$ addition versus urea---$O_2^{\bullet-}$ can be observed in the absence of amino acid moiety. Moreover, the thermodynamics of reaction of $O_2^{\bullet-}$ versus urea---$O_2^{\bullet-}$ to methylated-TyrO$^{\bullet}$ (ArO$^{\bullet}$) are shown in Scheme 2, Reactions I and J, respectively. The $O_2^{\bullet-}$ addition to Tyr-3 and Tyr-4 (Reaction I) only yielded dioxetane products but not in the presence of urea (Reaction J) which suggests the need for H-bond donors in the preferential formation of hydroperoxide. In general, a more consistent trend in relative reactivity of methylated– TyrO$^{\bullet}$ was observed similar to PhO$^{\bullet}$ in which urea---$O_2^{\bullet-}$ gave less endoergic (or more exoergic in the case of Tyr-2) free energies of reaction to Tyr-1, Tyr-3 and Tyr-4 relative to $O_2^{\bullet-}$ alone. These results further suggest that urea as well as carboxylic acid group can play a significant role in the facilitation of $O_2^{\bullet-}$ addition via α-effect.

Figure 8 shows the increase in hydroperoxide formation as a function of urea concentration consistent to that observed using arginine as H-bond donor (see Figure 2), while Figure 9 demonstrates the inverse relationship of the time of addition of urea on hydroperoxide formation. Although the yield of hydroperoxide with 1 mM tyrosine alone in Figure 8 is relatively lower, i.e ~ 0.3 μM, compared to ~ 0.6 μM using 1 mM of tyrosine as shown in

Figure 2c, the plot shows a qualitative trend of the dependence of the amount of hydroperoxide formed as a function of urea concentration. The dependence of hydroperoxide formation on the time of urea addition as well as on the concentration of urea further supports that urea can have a stabilizing effect on the hydroperoxide adduct or that the α-effect can enhance hydroperoxide formation. To shed more insights on to whether the enhanced production of hydroperoxide is mainly due to α-effect from urea, and/or stabilization of the TyrO-O_2H adduct by urea, the thermodynamics of urea addition to TyrO-O_2H was investigated. The addition of urea to TyrO-O_2H (Scheme 2, Reaction L), is less favored with $\Delta G_{rxn,aq,298K}$ = 13.0 kcal/mol compared to the addition of urea---$O_2^{\bullet-}$ to TyrO$^\bullet$ with $\Delta G_{rxn,aq,298K}$ = −3.7 kcal/mol (Scheme 2, Reaction J). Given the endoergicity of urea addition to TyrO-O_2H (Reaction L) versus urea---$O_2^{\bullet-}$ to TyrO$^\bullet$ (Reaction J), the latter is the most preferred pathway for urea-hydroperoxide complex formation. This trend is also true for all the methylated-TyrO$^\bullet$ analogues (see Scheme 2, Reaction J versus L). Based on the energetics of tyrosyl hydroperoxide formation presented thus far, it is therefore reasonable to assume that the hydroperoxide formed can be facilitated by H-bond donor via α-effect.

Conclusion

The role of α-effect on the enhancement of tyrosyl hydroperoxide formation has been experimentally and computationally explored. Superoxide exhibits various modes of H-bond interaction with carboxylic acid, amine and amide groups of amino acids as well as non-amino acids. Initial H-bonding of carboxylic acid and/or amine groups to $O_2^{\bullet-}$ causes polarization of the spin and charge density distribution around the $O_2^{\bullet-}$ resulting to a more favorable $O_2^{\bullet-}$ addition reaction with PhO$^\bullet$ or TyrO$^\bullet$ as shown by the less positive (or more negative) free energies of this reaction compared to in the absence of H-bond donors. Addition of $O_2^{\bullet-}$ to TyrO$^\bullet$ at the ortho-position is the most thermodynamically preferred mode of addition in the presence or absence of H-bond donor such as urea. The role of urea in either stabilizing the tyrosyl hydroperoxide adduct via H-bonding, or enhancing hydroperoxide formation through α-effect was computationally investigated using TyrO$^\bullet$ and its methylated analogues and results indicate that the latter is the more preferred mechanism. Therefore, in enzyme systems containing TyrO$^\bullet$, the presence of acidic moieties or H-bond donors at close proximity to TyrO$^\bullet$ may lead to the facilitation of hydroperoxide formation and hence potential enzyme inactivation. Site-directed mutagenesis may be able to shed more insights in to this phenomenon and merits further investigation. Moreover, the presence of exogenous H-bond donors such as urea or alcohols in elevated concentrations may induce hydroperoxide formation, and therefore, can play a pro-oxidant role in the initiation of oxidative stress in biological systems.

The models used in this study have provided new insights into the understanding of the molecular mechanism of oxidative damage as mediated by strong interaction of $O_2^{\bullet-}$ with H-bond donors. The implication of α-effect in hydroperoxide formation in various enzyme systems (23) containing protein radicals such as TyrO$^\bullet$ needs further investigation since there has been growing evidence on the pro-oxidant role of urea and its derivatives in the initiation of oxidative stress and damage in biological systems such as the inactivation of the R2 subunit of ribonucleotide reductase by hydroxyurea (20). Furthermore, increased production of reactive oxygen species, DNA damage, protein carbonylation levels, or increased expression of the oxidative stress-responsive transcription factor, Gadd153/CHOP, at the mRNA and protein levels in cultured renal cells have been observed during hyperosmolality caused by elevated concentrations of NaCl and urea, or during urea treatment (57). Further studies is also necessary on the potential implication of this hydroperoxide formation from tryptophan radical found in other enzyme systems (23).

Supplementary Material

Refer to Web version on PubMed Central for supplementary material.

Acknowledgement

This publication was made possible by grant number HL 81248 from the NIH National Heart, Lung, and Blood Institute. This work was supported in part by an allocation of computing time from the Ohio Supercomputer Center.

References

1. Halliwell, B.; Gutteridge, JMC. Free Radicals in Biology and Medicine. Vol. 4th ed.. New York: Oxford University; 2007.
2. Choksi KB, Boylston WH, Rabek JP, Widger WR, Papaconstantinou J. Oxidatively damaged proteins of heart mitochondrial electron transport complexes. Biochim. Biophys. Acta, Mol. Basis Dis 2004;1688:95–101.
3. Green MR, Hill HAO, Okolowzubkowska MJ, Segal AW. The production of hydroxyl and superoxide radicals by stimulated human neutrophils - measurements by EPR spectroscopy. FEBS Lett 1978;100:23–26. [PubMed: 220087]
4. Valdez LB, Boveris A. Nitric oxide and superoxide radical production by human mononuclear leukocytes. Antioxid. Redox Signaling 2001;3:505–513.
5. Bielski BHJ, Cabelli DE, Arudi RL. Reactivity of HO_2/O_2^- radicals in aqueous solution. J. Phys. Chem. Ref. Data 1985;14:1041–1100.
6. Locigno EJ, Zweier JL, Villamena FA. Nitric oxide release from the decomposition of the superoxide radical anion adduct of cyclic nitrones in aqueous medium. Org. Biomol. Chem 2005;3:3220–3227. [PubMed: 16106305]
7. Villamena FA, Hadad CM, Zweier JL. Comparative DFT study of the spin trapping of methyl, mercapto, hydroperoxy, superoxide, and nitric oxide radicals by various substituted cyclic nitrones. J. Phys. Chem. A 2004;109:1662–1674. [PubMed: 16833491]
8. Villamena FA, Hadad CM, Zweier JL. Theoretical study of the spin trapping of hydroxyl radical by cyclic nitrones: A density functional theory approach. J. Am. Chem. Soc 2004;126:1816–1829. [PubMed: 14871114]
9. Villamena FA, Merle JK, Hadad CM, Zweier JL. Rate constants of hydroperoxyl radical addition to cyclic nitrones: A DFT study. J. Phys. Chem. A 2007;111:9995–10001. [PubMed: 17845014]
10. Villamena FA, Xia S, Merle JK, Lauricella R, Tuccio B, Hadad CM, Zweier JL. Reactivity of superoxide radical anion with cyclic nitrones: Role of intramolecular H-bond and electrostatic effects. J. Am. Chem. Soc 2007;129:8177–8191. [PubMed: 17564447]
11. Villamena FA, Zweier JL. Detection of reactive oxygen and nitrogen species by EPR spin trapping. Antioxid. Redox Signaling 2004;6:619–629.
12. Beal MF. Oxidatively modified proteins in aging and disease. Free Radical Biol. Med 2002;32:797–803. [PubMed: 11978481]
13. Gaudu P, Niviere V, Petillot Y, Kauppi B, Fontecave M. The irreversible inactivation of ribonuclease reductase from E. Coli by superoxide radicals. FEBS Lett 1996;387:137–140. [PubMed: 8674535]
14. Sohal RS. Role of oxidative stress and protein oxidation in the aging process. Free Radical Biol. Med 2002;33:37–44. [PubMed: 12086680]
15. d'Alessandro N, Bianchi G, Fang X, Jin F, Schuchmann H, Sonntag CV. Reaction of superoxide with phenoxyl-type radicals. J. Chem. Soc 2000;2:1862–1867.
16. Fang X, Jin F, Jin H, Sonntag CV. Reaction of the superoxide radical with the N-centered radical derived from N-acetyltryptophan methyl ester. J. Chem. Soc 1998;2:259–263.
17. Winterbourn CC, Kettle AJ. Radical-radical reactions of superoxide: a potential route to toxicity. Biochem. Biophys. Res. Commun 2003;305:729–736. [PubMed: 12763053]
18. Winterbourn CC, Metodiewa D. Reactivity of biologically important thiol compounds with superoxide and hydrogen peroxide. Free Radical Biol. Med 1999;27:322–328. [PubMed: 10468205]

19. Winterbourn CC, Parsons-Mair HN, Gebicki S, Gebicki JM, Davies MJ. Requirements for superoxide-dependent tyrosine hydroperoxide formation in peptides. Biochem. J 2004;381:241–248. [PubMed: 15025556]
20. Jordan A, Reichard P. Ribonucleotide Reductases. Annu. Rev. Biochem 1998;67:71–98. [PubMed: 9759483]
21. Reece SY, Seyedsayamdost MR, Stubbe J, Nocera DG. Direct observation of a transient tyrosine radical competent for initiating turnover in a photochemical ribonucleotide reductase. J. Am. Chem. Soc 2007;129:13828–13830. [PubMed: 17944464]
22. Yun D, Saleh L, Garcia-Serres R, Chicalese BM, An YH, Huynh BH, Bollinger JM Jr. Addition of oxygen to the diiron (II/II) cluster is the slowest step in formation of the tyrosyl radical in the W103Y variant of ribonucleotide reductase protein R2 from mouse. J. Am. Chem. Soc 2007;46:13067–13073.
23. Stubbe J, van der Donk WA. Protein radicals in enzyme catalysis. Chem. Rev 1998;98:705–762. [PubMed: 11848913]
24. Detweiler CD, Lardinois OM, Deterding LJ, Ortiz de Montellano PR, Tomer KB, Mason RP. Identification of the myoglobin tyrosyl radical by immuno-spin trapping and its dimerization. Free Radical Biol. Med 2005;38:969–976. [PubMed: 15749393]
25. McCormick ML, Gaut JP, Lini T-S, Britigan BE, Buettner GR, Heinecke JW. Electron paramagnetic resonance detection of free tyrosyl radical generated by myeloperoxidase, lactoperoxidase, and horseradish peroxidase. J. Biol. Chem 1998;273:32030–32037. [PubMed: 9822676]
26. Fukuzawa K, Fujisaki A, Akai K, Tokumura A, Terao J, Gebicki JM. Measurement of phosphatidylcholine hydroperoxides in solution and intact membranes by the ferric-xylenol orange assay. Anal. Biochem 2006;359:18–25. [PubMed: 17049475]
27. Nourooz-Zadeh J, Tajaddini-Sarmadi J, Wolff SP. Measurement of plasma hydroperoxide concentration by the ferrous oxidation-xylenol orange assay in conjunction with triphenylphosphine. Anal. Biochem 1994;220:403–409. [PubMed: 7978285]
28. Spartan'04. Irvine, CA: Wavefunction, Inc.; 2004.
29. Krenske EH, Schiessera CH. A comparison of orbital interactions in the additions of phosphonyl and acyl radicals to double bonds. Org. Biomol. Chem 2008;6:854–859. [PubMed: 18292876]
30. Violi A, Truong TN, Sarofim AF. Kinetics of hydrogen abstraction reactions from polycyclic aromatic hydrocarbons by H atoms. J. Phys. Chem. A 2004;108:4846–4852.
31. Labanowski, JK.; Andzelm, JW., editors. Density Functional Methods in Chemistry. New York: Springer-Verlag; 1991.
32. Parr, RG.; Yang, W. Density-functional Theory of Atoms and Molecules. New York: Clarendon Press; 1989.
33. Becke AD. Density-functional exchange-energy approximation with correct asymptotic behavior. Phys. Rev. A 1988;38:3098–3100. [PubMed: 9900728]
34. Becke AD. A new mixing of Hartree-Fock and local-density-functional theories. J. Chem. Phys 1993;98:1372–1377.
35. Hehre, WJ.; Radom, L.; Schleyer, PV.; Pople, JA. Ab Initio Molecular Orbital Theory. New York: John Wiley & Sons; 1986.
36. Lee C, Yang W, Parr RG. Development of the Colle-Salvetti correlation-energy formula into a functional of the electron density. Phys. Rev. B 1988;37:785–789.
37. Frisch, MJTGW.; Schlegel, HB.; Scuseria, GE.; Robb, MA.; Cheeseman, JR.; Montgomery, JA., Jr; Vreven, T.; Kudin, KN.; Burant, JC.; Millam, JM.; Iyengar, SS.; Tomasi, J.; Barone, V.; Mennucci, B.; Cossi, M.; Scalmani, G.; Rega, N.; Petersson, GA.; Nakatsuji, H.; Hada, M.; Ehara, M.; Toyota, K.; Fukuda, R.; Hasegawa, J.; Ishida, M.; Nakajima, T.; Honda, Y.; Kitao, O.; Nakai, H.; Klene, M.; Li, X.; Knox, JE.; Hratchian, HP.; Cross, JB.; Bakken, V.; Adamo, C.; Jaramillo, J.; Gomperts, R.; Stratmann, RE.; Yazyev, O.; Austin, AJ.; Cammi, R.; Pomelli, C.; Ochterski, JW.; Ayala, PY.; Morokuma, K.; Voth, GA.; Salvador, P.; Dannenberg, JJ.; Zakrzewski, VG.; Dapprich, S.; Daniels, AD.; Strain, MC.; Farkas, O.; Malick, DK.; Rabuck, AD.; Raghavachari, K.; Foresman, JB.; Ortiz, JV.; Cui, Q.; Baboul, AG.; Clifford, S.; Cioslowski, J.; Stefanov, BB.; Liu, G.; Liashenko, A.; Piskorz, P.; Komaromi, I.; Martin, RL.; Fox, DJ.; Keith, T.; Al-Laham, MA.; Peng, CY.; Nanayakkara, A.; Challacombe, M.; Gill, PMW.; Johnson, B.; Chen, W.; Wong, MW.; Gonzalez, C.; Pople, JA. Gaussian 03. Pittsburgh PA: Gaussian, Inc; 2003.

38. Reed AE, Curtiss LA, Weinhold F. Intermolecular interactions from a natural bond orbital, donor-acceptor viewpoint. Chem. Rev 1988;88:899–926.
39. Barone V, Cossi M, Tomasi J. A new definition of cavities for the computation of solvation free energies by the polarizable continuum model. J. Chem. Phys 1997;107:3210–3221.
40. Barone V, Cossi M, Tomasi J. Geometry optimization of molecular structures in solution by the polarizable continuum model. J. Comput. Chem 1998;19:404–417.
41. Cossi M, Barone V, Cammi R, Tomasi J. Ab initio study of solvated molecules: a new implementation of the polarizable continuum model. Chem. Phys. Lett 1996;255:327–335.
42. Tomasi J, Mennucci B, Cammi R. Quantum mechanical continuum solvation models. Chem. Rev 2005;105:2999–3093. [PubMed: 16092826]
43. Tomasi J, Persico M. Molecular interactions in solution: An overview of methods based on continuous distributions of the solvent. Chem. Rev 1994;94:2027–2094.
44. Scott AP, Radom L. Harmonic vibrational frequencies: An evaluation of Hartree-Fock, Moeller-Plesset, quadratic configuration interaction, density functional theory, and semiempirical scale factors. J. Phys. Chem 1996;100:16502–16513.
45. Jin F, Leitich J, von Sonntag C. The superoxide radical reacts with tyrosine-derived phenoxyl radicals by addition rather than electron transfer. J. Chem. Soc., Perkin Trans 1993;29:1583–1588.
46. Issacs, NS. Physical Organic Chemistry. Essex, England: Longman Scientific and Technical; 1987.
47. Ren Y, Yamataka H. The alpha-effect in gas-phase S_N2 reactions: Existence and the origin of the effect. J. Org. Chem 2007;72:5660–5667. [PubMed: 17590049]
48. Buettner GR. The pecking order of free radicals and antioxidants: Lipid peroxidation, α-tocopherol and ascorbate. Arch. Biochem. Biophys 1993;300:535–543. [PubMed: 8434935]
49. Ormo M, Regnstrom K, Wang Z, Que L, Sahlin M, Sjoberg BM. Residues important for radical stability in ribonucleotide reductase from Escherichia coli. J. Biol. Chem 1995;270:6570–6576. [PubMed: 7896794]
50. Koppenol, WH. Oxidases and Related Redox Systems. Oxford: Pergamon Press; 1982.
51. Fridovich I. Oxygen toxicity: A radical explanation. J. Exptl. Biol 1998;201:1203–1209. [PubMed: 9510531]
52. Benovic J, Tillman T, Cudd A, Fridovich I. Electrostatic facilitation of the reaction catalyzed by the manganese-containing and the iron-containing superoxide dismutases. Arch. Biochem. Biophys 1983;221:329–332. [PubMed: 6340608]
53. Cudd A, Fridovich I. Electrostatic interactions in the reaction mechanism of bovine erythrocyte superoxide dismutase. J. Biol. Chem 1982;257:11443–11447. [PubMed: 7118890]
54. Getzoff ED, Cabelli DE, Fisher CL, Parge HE, Viezzzoli MS, Banci L, Hallewell RA. Faster superoxide dismutase mutants designed by enhancing electrostatic guidance. Nature 1992;358:347–351. [PubMed: 1353610]
55. Behar D, Czapski G, Rabani J, Dorfman LM, Schwarz HA. Acid dissociation constant and decay kinetics of the perhydroxyl radical. J. Phys. Chem 1970;74:3209–3213.
56. Czapski G, Bielski BHJ. The formation and decay of H_2O_3 and HO_2 in electron-irradiated aqueous solutions. J. Phys. Chem 1963;67:2180–2184.
57. Kueltz D. Hyperosmolality triggers oxidative damage in kidney cells. Proc. Nat. Acad. Sci. U.S.A 2004;101:9177–9178.

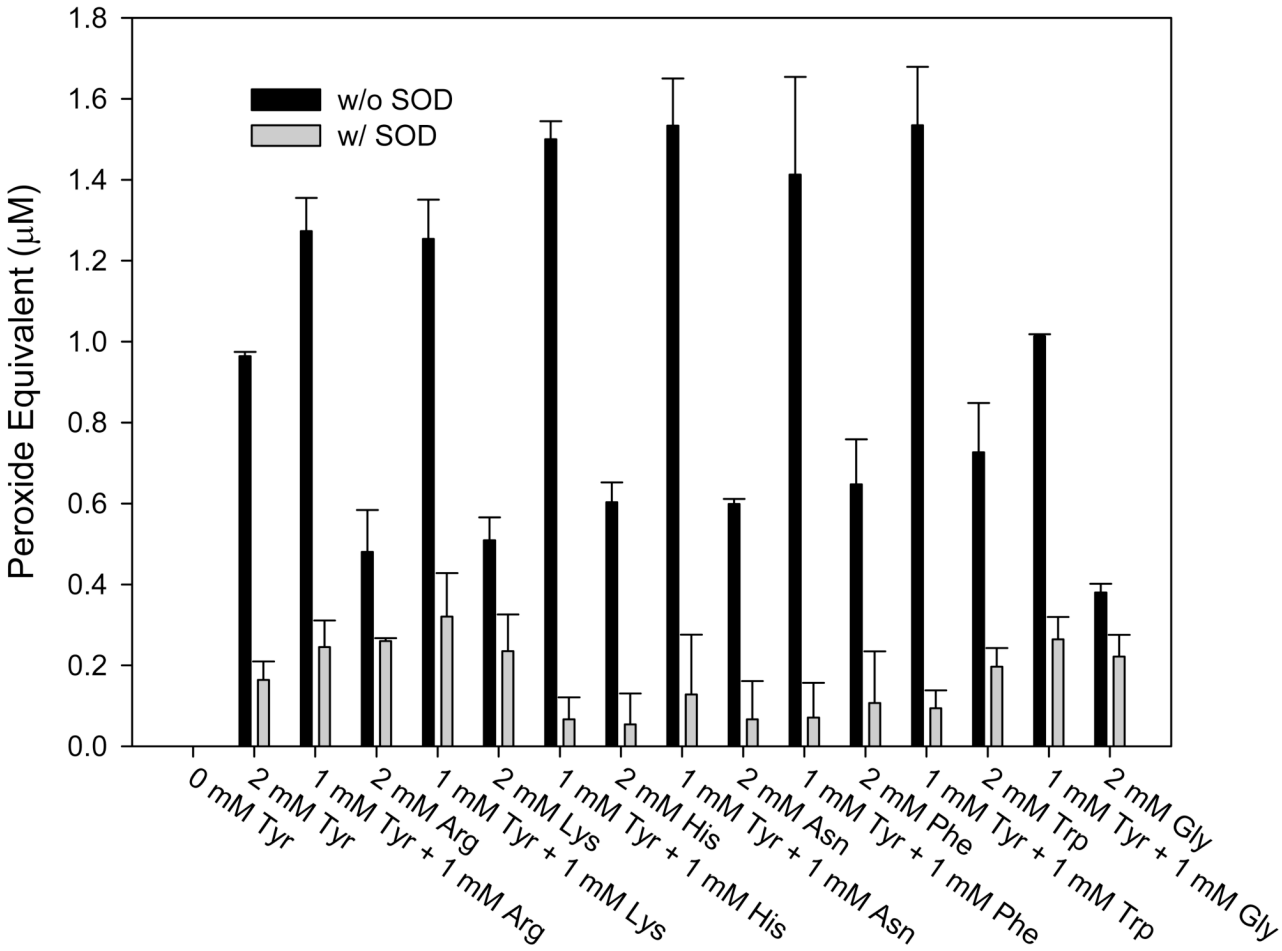

Figure 1.

Tyrosyl hydroperoxide formation from tyrosine (1 mM) and an amino acid (1 mM) in the presence (gray) and absence (black) of SOD (20 μg/mL). For an amino acid alone, 2 mM concentration was used. Each solution contains horseradish peroxidase (HPO) (10 μg/mL), xanthine oxidase (XO) (0.05 U/mL), acetaldehyde (1 mM) and catalase (20 μg/mL) in 10 mM phosphate buffer solution. Hydroperoxide concentration was analyzed using FOX assay. All data were corrected relative to the peroxide equivalent calculated in the absence of amino acid (shown as -Tyr). Plots are means ± SD. See general experimental section for details.

(a)

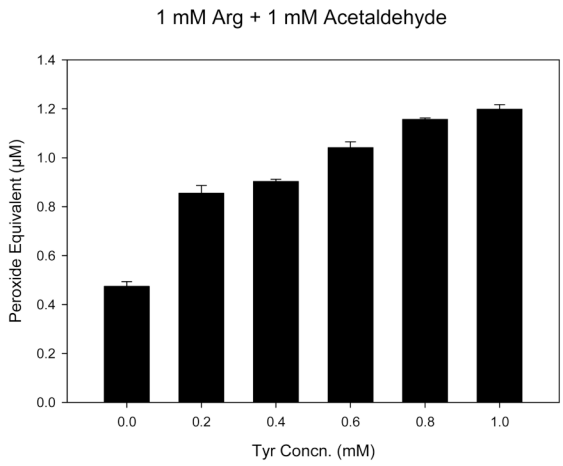

(b)

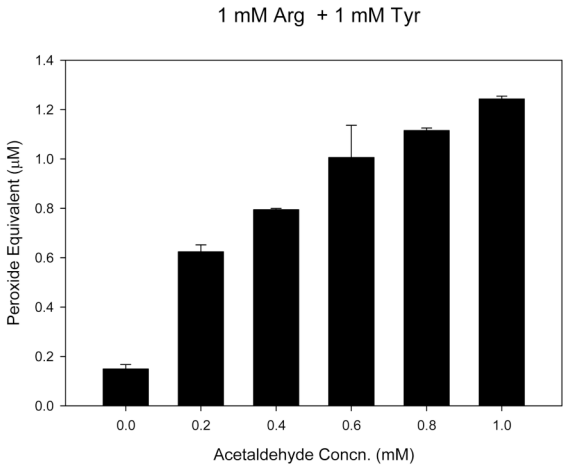

(c)

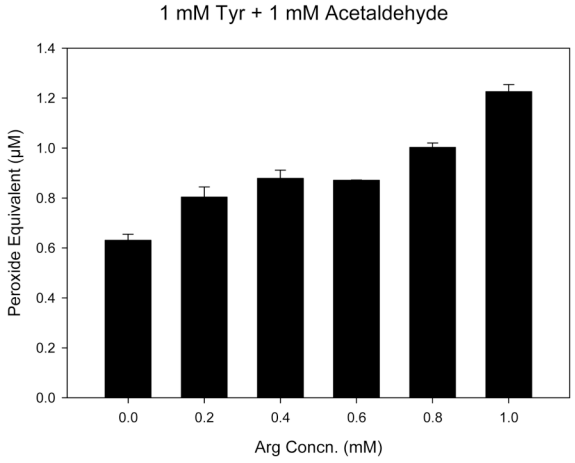

Figure 2.

Dependence of hydroperoxide formation as a function of (a) tyrosine; (b) acetaldehyde; or (c) arginine concentrations (0–1.0 mM) at constant horseradish peroxidase (HPO) (10 μg/mL), xanthine oxidase (XO) (0.05 U/mL), and catalase (20 μg/mL) concentrations. Hydroperoxide concentration was analyzed using FOX assay. All data were corrected relative to the peroxide equivalent calculated in the absence of amino acid. Plots are means ± SD. See general experimental section for details.

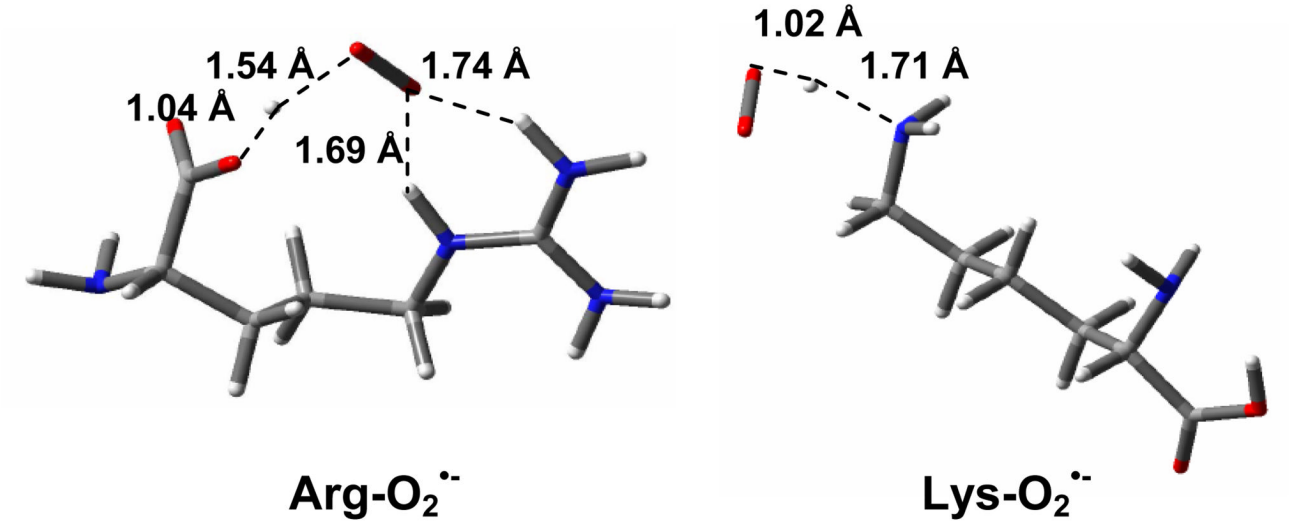

Figure 3.
Optimized structures at the B3LYP/6-31G* level of theory of superoxide radical anion complexes with arginine (left) and lysine (right) showing the intermolecular H-bonding interaction.

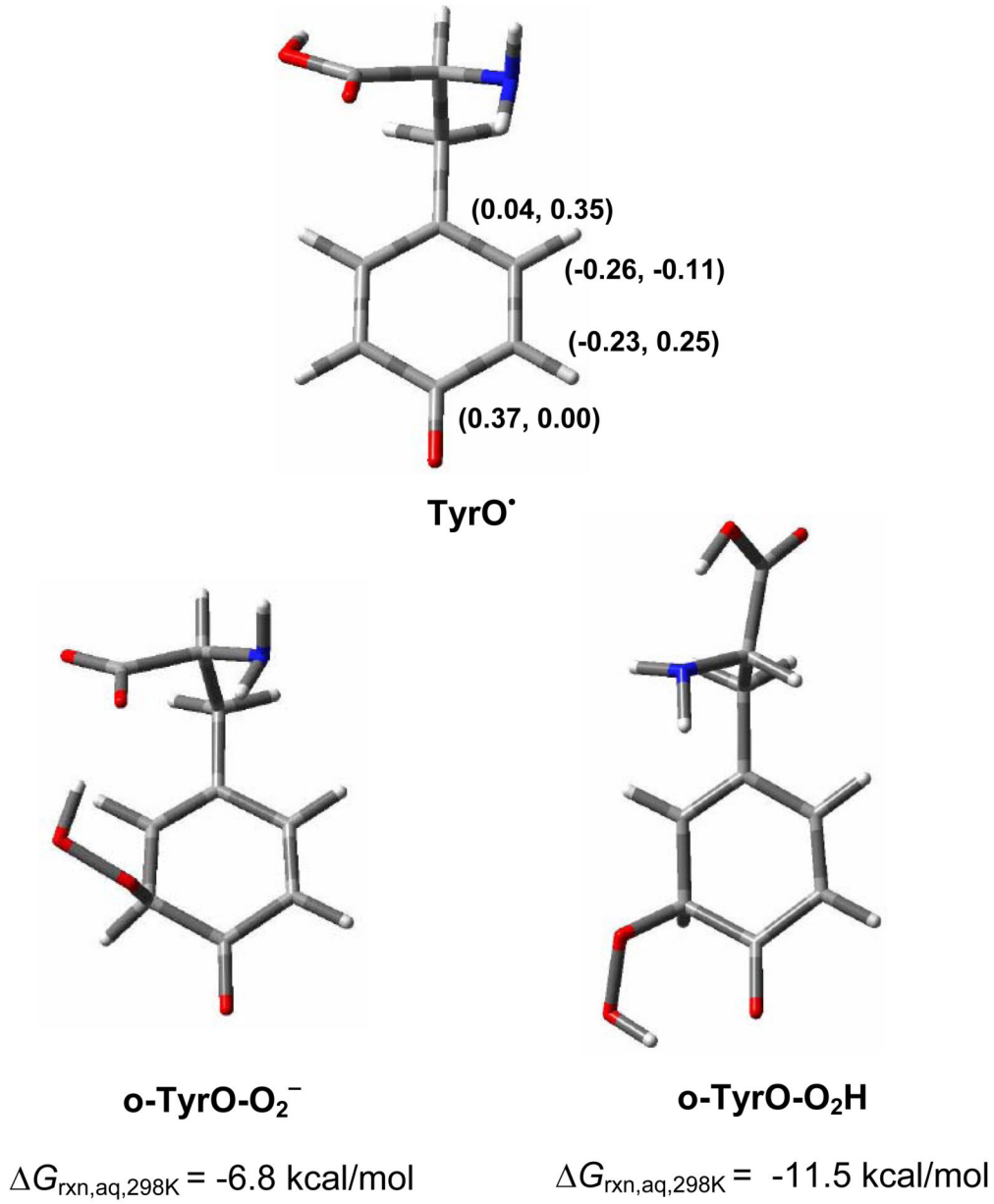

Figure 4.
Charge and spin density (in e) distributions on the aromatic carbon atoms of TyrO• at the PCM/B3LYP/6-31+G**//B3LYP/6-31G* level of theory and the free energies of reaction ($\Delta G_{rxn,aq,298K}$) for the formation of the tyrosyl peroxide (ortho-TyrO-O_2^-) and hydroperoxide (ortho-TyrO-O_2H) adducts.

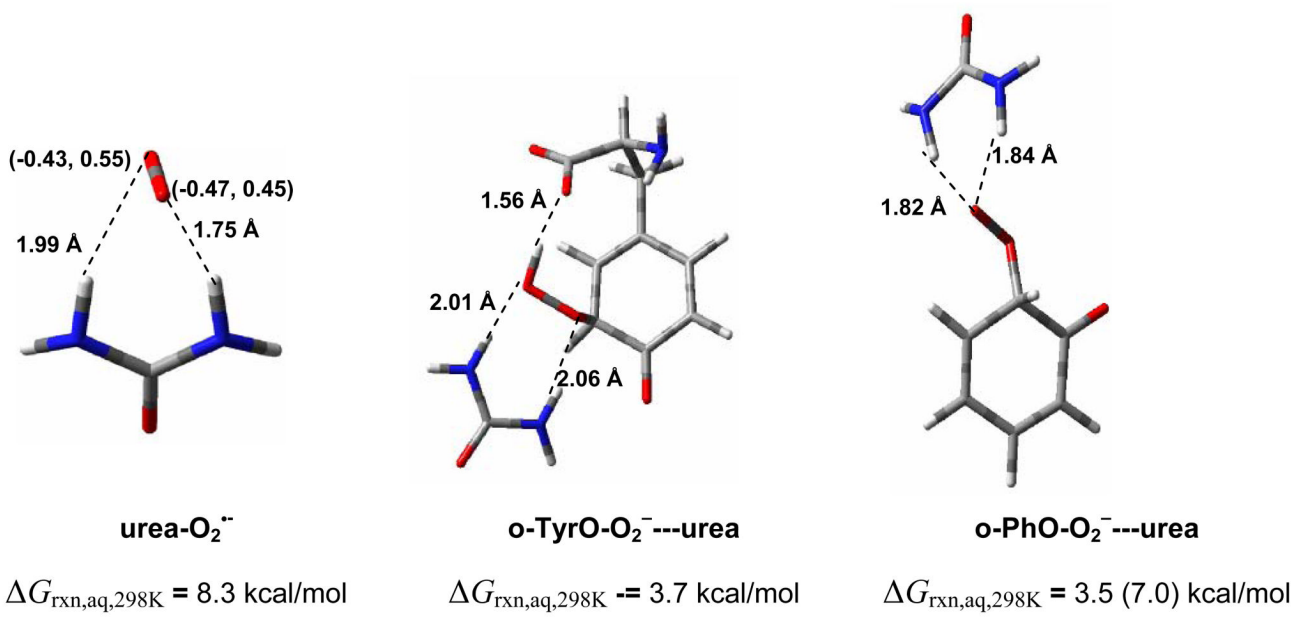

Figure 5.
Free energies of reaction ($\Delta G_{rxn,aq,298K,}$ in kcal/mol) for the formation of Tyr-OO^{-}---urea, o-TyrO-O_2^{-}---urea-and o-PhO-O_2^{-}---urea (value in parentheses is in the absence of urea).

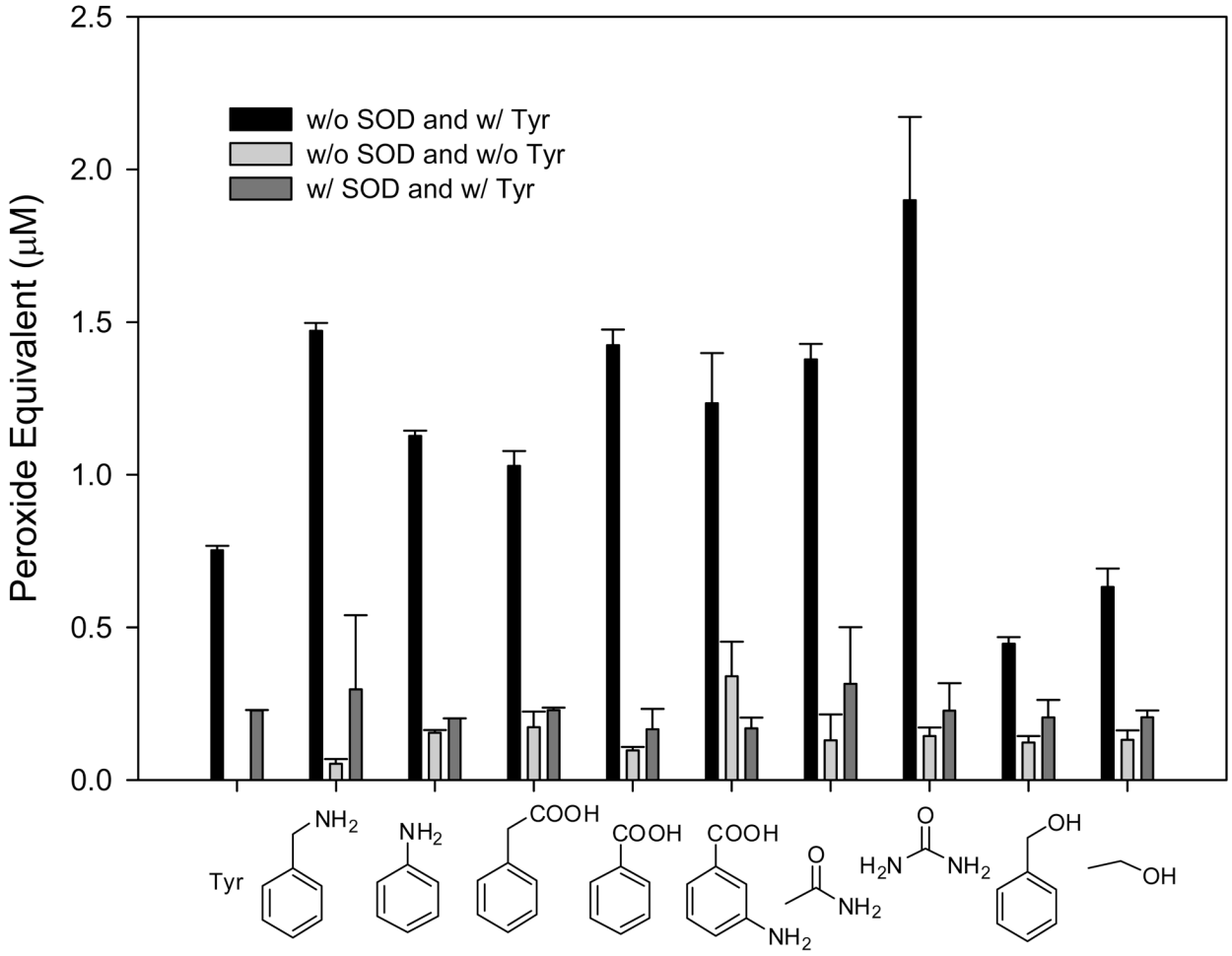

Figure 6.

Tyrosyl hydroperoxide formation with H-bond donating non-amino acids (1 mM), tyrosine (1 mM), horseradish peroxidase (HPO) (10 μg/mL), xanthine oxidase (XO) (0.05 U/mL), acetaldehyde (1 mM) and catalase (20 μg/mL) in 10 mM phosphate buffer solution in the presence (dark gray), or absence (black) of SOD (20 μg/mL) and in the absence of tyrosine (light gray). A concentration of 2 mM was used for tyrosine in the absence of non-amino acid. All data were corrected relative to the peroxide equivalent calculated in the absence of amino acid (shown as -Tyr). Plots are means ± SD. See general experimental section for details.

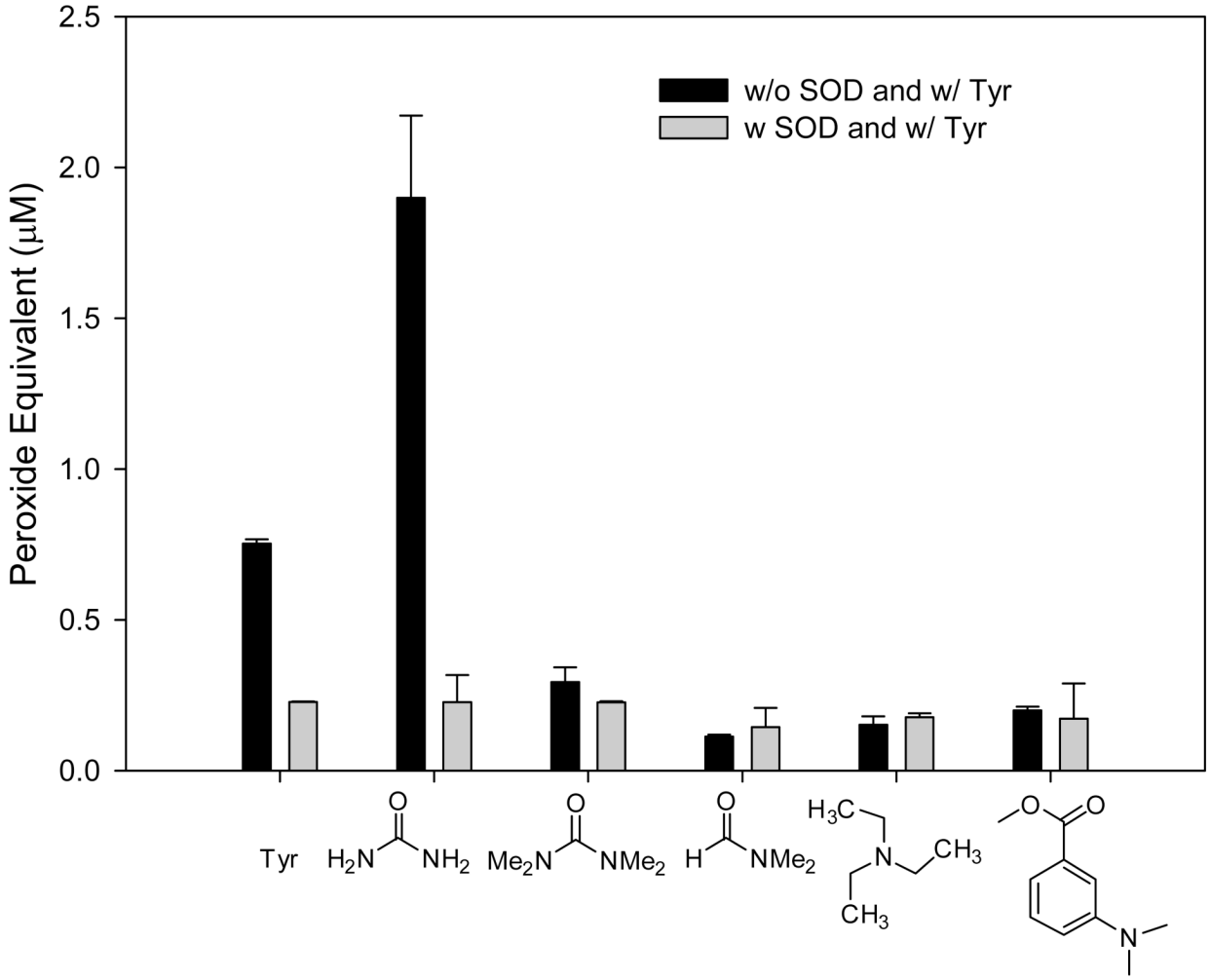

Figure 7.

Tyrosyl hydroperoxide formation with non-amino acids (1 mM) in the absence of H-bond donors, tyrosine (1 mM), horseradish peroxidase (HPO) (10 μg/mL), xanthine oxidaese (XO) (0.05 U/mL), acetaldehyde (1 mM) and catalase (20 μg/mL) in 10 mM phosphate buffer solution in the presence (gray) and absence (black) of SOD (20 μg/mL). A concentration of 2 mM was used for tyrosine in the absence of non-amino acid. All data were corrected relative to the peroxide equivalent calculated in the absence of amino acid as no peroxide equivalent. Plots are means ± SD. See general experimental section for details.

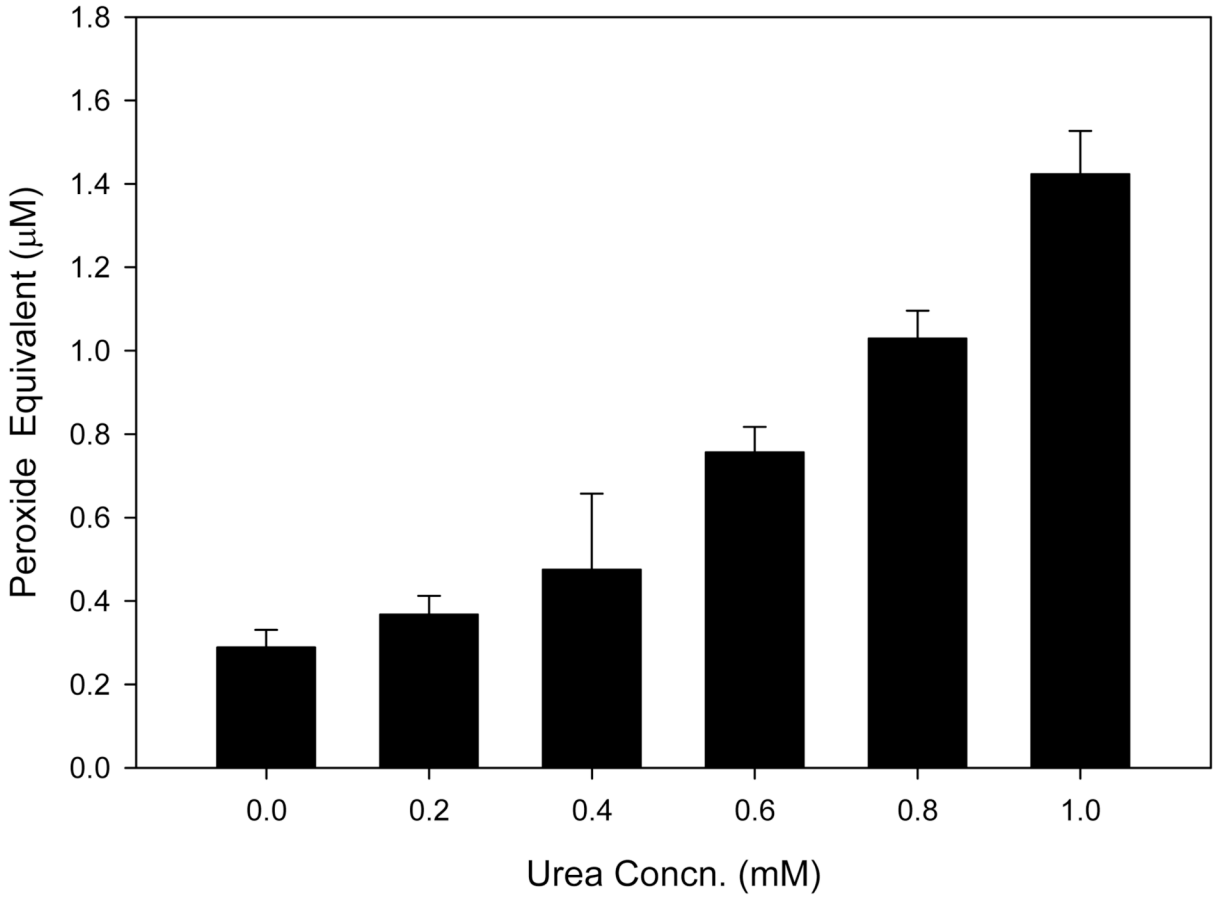

Figure 8.
Hydroperoxide formation as a function of urea concentration (0.0–1.0 mM) in the presence of 1 mM tyrosine, horseradish peroxidase (HPO) (10 μg/mL), xanthine oxidase (XO) (0.05 U/mL), acetaldehyde (1 mM) and catalase (20 μg/mL) in 10 mM phosphate buffer solution. All data were corrected relative to the peroxide equivalent calculated in the absence of amino acid as no peroxide equivalent. Plots are means ± SD. See experimental section for details.

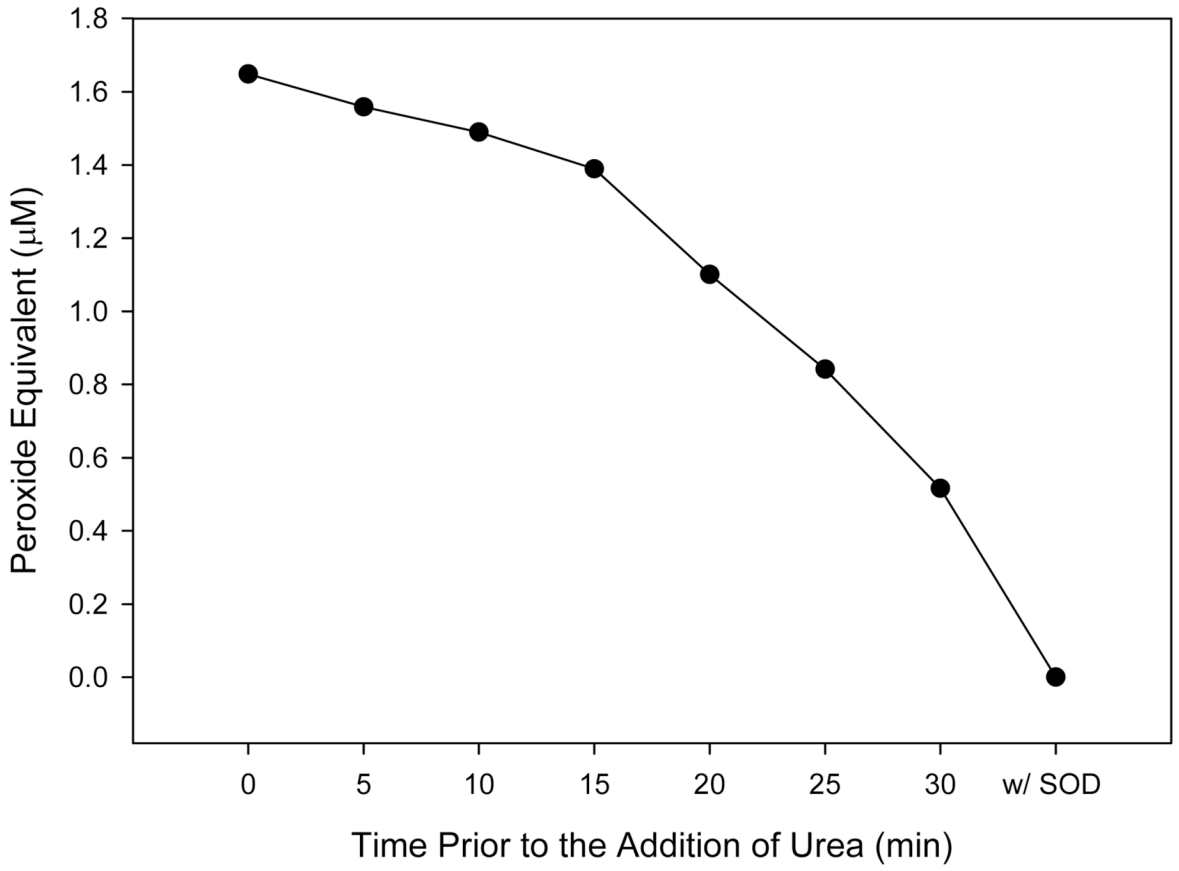

Figure 9.
Effect of time of addition of urea on the hydroperoxide formation in the presence of 1 mM tyrosine, horseradish peroxidase (HPO) (10 μg/mL), xanthine oxidase (XO) (0.05 U/mL), acetaldehyde (1 mM) and catalase (20 μg/mL) in 10 mM phosphate buffer solution. All data were corrected relative to the peroxide equivalent calculated in the absence of amino acid as no peroxide equivalent. See experimental section for details.

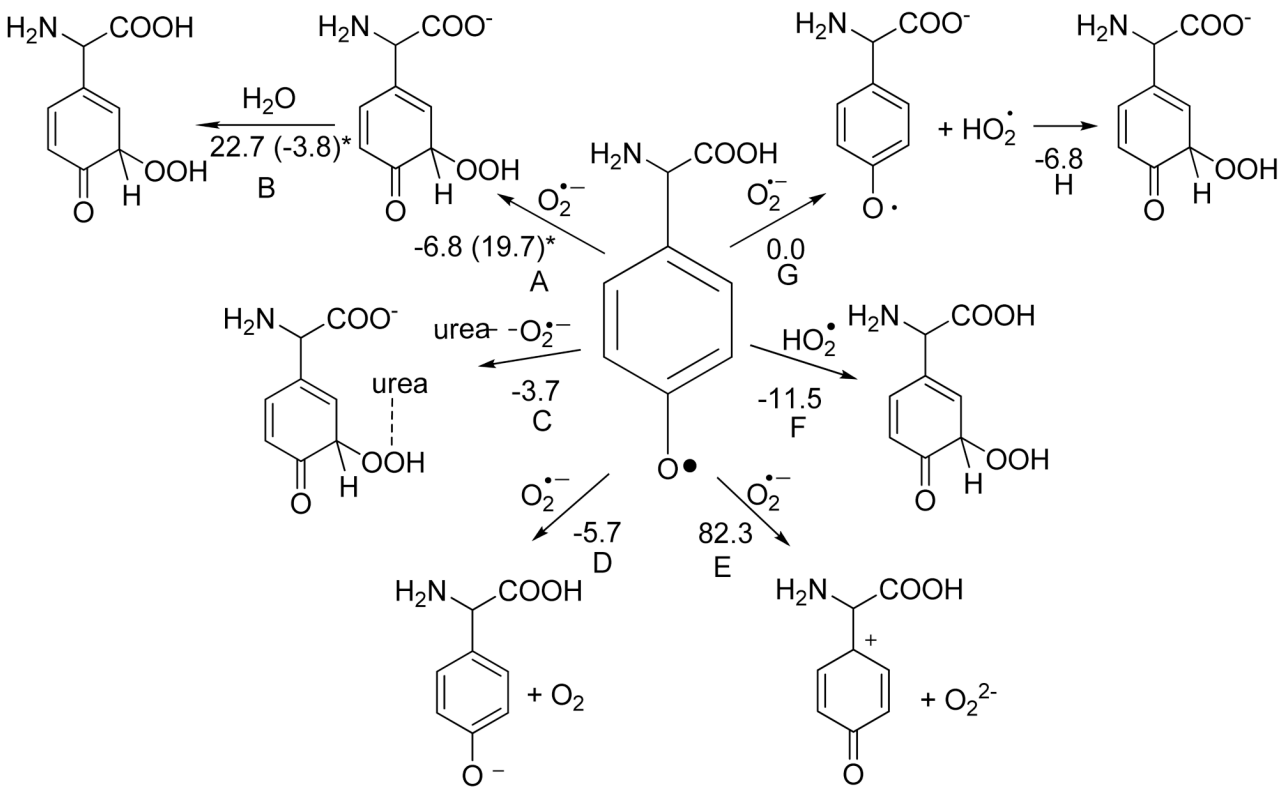

Scheme 1.

Modes of tyrosyl $O_2^{\bullet -}$ and $HO_2^{\bullet}$ adduct formation and their respective free energies of reaction in aqueous phase $\Delta G_{rxn,aq,298K}$ (kcal/mol). *For reaction A, value in parenthesis represents $O_2^{\bullet -}$addition without proton transfer from the carboxylic acid group to the peroxide. For reaction B, value in parenthesis represents proton abstraction of peroxide from water.

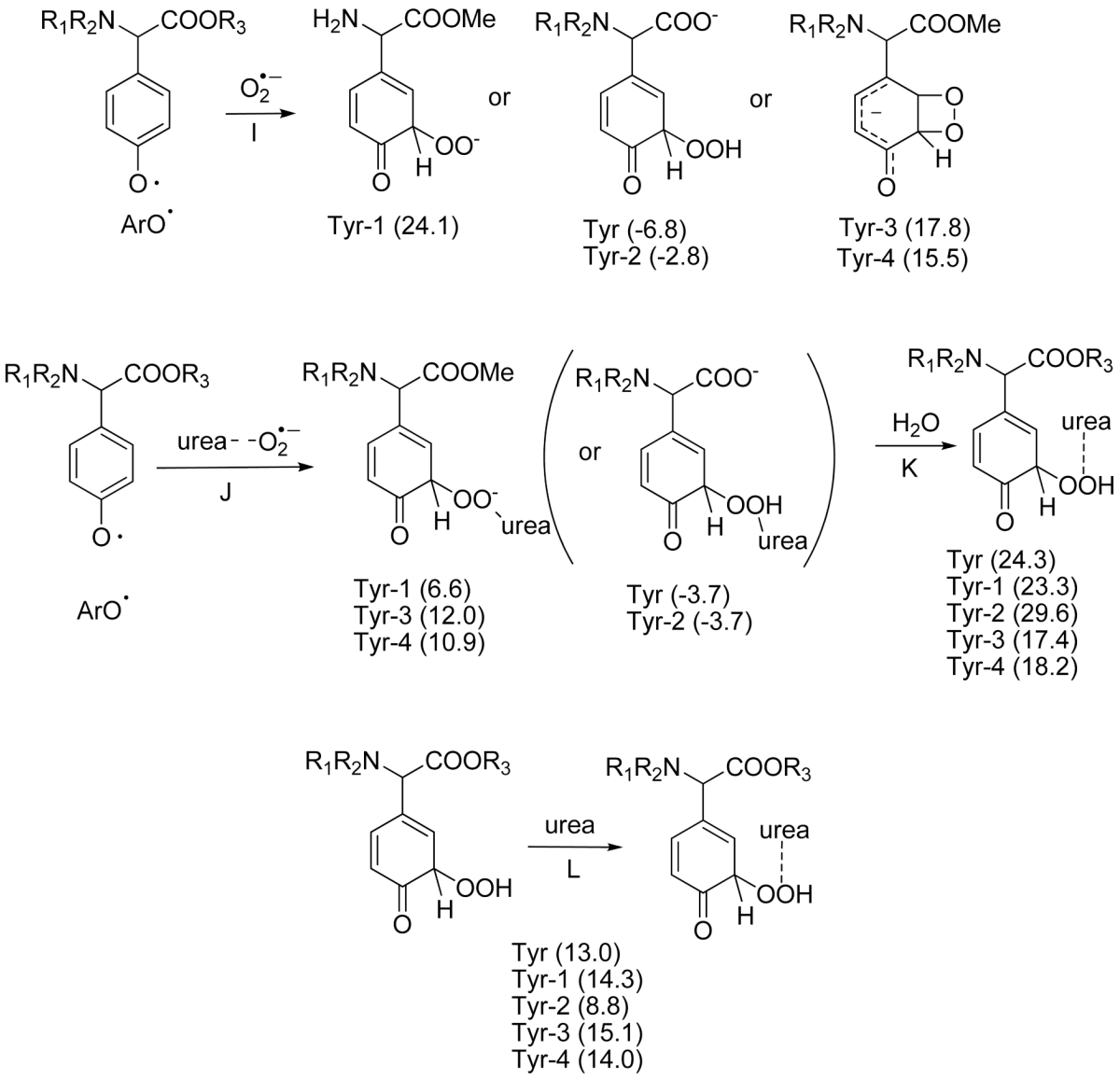

Scheme 2.

Modes of methylated-tyrosyl $O_2^{\bullet-}$ and $HO_2^{\bullet}$ adduct formation and their respective free energies of reaction in aqueous phase $\Delta G_{rxn,aq,298K}$ (kcal/mol). Tyr: $R_1 = R_2 = R_3 = H$; Tyr-1: $R_1 = R_2 = H$; $R_3 = Me$; Tyr-2: $R_1 = R_2 = Me$; $R_3 = H$; Tyr-3: $R_1 = H$; $R_2 = R_3 = Me$; Tyr-4: $R_1 = R_2 = R_3 = Me$.

Table 1

Free energies of complexation of superoxide radical anion with amino acids and their respective spin and charge density distribution at the PCM/B3LYP/6-31+G**//B3LYP/6-31G* level of theory at 298 K.

Entry	$\Delta G_{rxn,298K,aq}$ (kcal/mol)	$\Delta H_{rxn,298K,aq}$ (kcal/mol)	Spin density (e)		Charge density (e)	
			α–O[c]	β–O[c]	α–O[c]	β–O[c]
$O_2^{\bullet-}$	n/a	n/a	0.50	0.50	−0.50	−0.50
$HO_2^{\bullet}$	n/a	n/a	0.73	0.27	−0.15	−0.35
Arg--$O_2^{\bullet-}$	−0.5	−10.0	0.48	0.52	−0.41	−0.36
Lys--$O_2^{\bullet-}$[a]	−2.4	−9.9	0.70	0.30	−0.21	−0.38
His--$O_2^{\bullet-}$	8.2	−3.0	0.50	0.50	−0.40	−0.41
Trp--$O_2^{\bullet-}$	5.1	−4.2	0.64	0.37	−0.27	−0.38
Asn--$O_2^{\bullet-}$	3.5	−5.2	0.67	0.34	−0.25	−0.38
Phe--$O_2^{\bullet-}$	2.9	−6.2	0.58	0.43	−0.35	−0.41
Gln--$O_2^{\bullet-}$	7.2	−2.7	0.66	0.34	−0.25	−0.38
Gly--$O_2^{\bullet-}$	13.6	4.7	0.50	0.50	−0.46	−0.45
Gly--$O_2^{\bullet-}$[b]	1.5	−5.8	0.66	0.35	−0.27	−0.39

[a] Proton transfer from ammonium to $O_2^{\bullet-}$.

[b] Proton transfer from carboxylic acid to $O_2^{\bullet-}$.

[c] α–O and β–O are the oxygen atoms that are farther and closer to a hydrogen atom, respectively.